Semi-Adaptive Beamforming for Co-Prime Circular Microphone Arrays

Jiahong Zhao and Christian Ritz
School of Electrical, Computer and Telecommunications Engineering, University of Wollongong, NSW, Australia
E-mail: jz262@uowmail.edu.au and critz@uow.edu.au

Abstract—**This paper proposes a semi-adaptive beamforming (SAB) algorithm for the co-prime circular microphone array (CPCMA), which takes advantage of subarray-based adaptive beamforming to achieve an optimised overall beampattern. The SAB approach calculates the bearings of grating lobes or the largest side lobes in the first sub-array before setting nulls at these directions in the beampattern of the second sub-array, aiming at removing the largest amplifications of undesired sources in the first beampattern. Compared with state-of-the-art co-prime array adaptive beamforming methods, the SAB considers the beamformer weights for each sub-array separately before combining them and generating the overall microphone array output, which fully utilises the co-prime property. Simulations indicate that the SAB improves the beampattern and array gain (AG) at low frequencies, which are dominant components of the speech energy, whilst maintaining equivalent results to the conventional CPCMA at high frequencies, leading to overall better performances in terms of beampattern and AG.**

I. INTRODUCTION

Designing a microphone array for speech sources processing entails a trade-off between obtaining adequate directivity at low frequencies, whilst avoiding spatial aliasing at high frequencies [1]. Processing of the microphone array recordings using beamforming is typically used to obtain an enhanced recording of the target signal whilst suppressing the effect of unwanted noise and other interfering sources. While the performance of the beamformer can improve by increasing the number of microphones and size of the array, this is often impractical for speech applications.

The co-prime microphone array (CPMA) possesses a beampattern with a narrower main lobe and less side lobes than an array that uses with the same number of microphones that are linearly spaced. The CPMA consists of two smaller sub-arrays whose beampatterns result in grating lobes for source signal frequencies above their spatial Nyquist frequency that is a function of the sub-array microphone number and spacing. The co-prime relationship between the number of microphones in each sub-array means that these grating lobes are offset spatially. Hence, joint processing of the sub-array outputs leads to suppression of the grating lobes and allows an increase in the spatial Nyquist frequency comparable with that of a similar sized array with many more microphones [2-4]. A number of papers have investigated applications that take advantage of co-prime arrays including the estimation of the direction of arrival (DOA) and the spatial power spectral density (PSD) [5-8].

Recent work [9] adapts the CPMA to a circular arrangement to form the co-prime circular microphone array (CPCMA), which achieves improved beampatterns and array gain (AG) results at high frequencies compared to a conventional Uniform Circular Array (UCA). However, conventional co-prime arrays utilising fixed-beamforming methods suffer from large side lobes in the overall beampattern, leading to a performance degradation in terms of AG at low frequencies. Semi-coprime arrays have been proposed and investigated to further cancel these side lobes [10-11], but the low-frequency performance could still be improved. Note that the semi-coprime array is a new type of sensor arrays, whilst the semi-adaptive beamforming proposed in this paper is a different term, applying adaptive beamforming approaches to only one sub-array of co-prime arrays.

Adaptive beamforming techniques have been applied to co-prime arrays to optimise the weights of the beamformer, and achieve better performance. The approach of [12] generates a much longer virtual uniform linear array (ULA) to compressively sample the signal before applying the principle of the minimum variance distortionless response (MVDR) beamformer to design an adaptive beamformer for the co-prime array. C. Liu and P. P. Vaidyanathan [13] also propose co-prime joint angle-Doppler estimation (co-prime JADE) to improve the degree-of-freedom (DOF) of co-prime arrays, whereas the above methods target obtaining a single set of overall beamforming weights corresponding to all microphones and do not explore the sub-array properties first. The work by Zhou et al [14] estimates the co-prime MVDR beamformer with the assistance of DOA cues of each sub-array, whereas the adaptive weights are also calculated for all microphones without combining sub-arrays. This paper explores a new path in co-prime adaptive beamforming to fully utilise the property of the co-prime arrangement, which is based on sub-array weighting and is not considered in the aforementioned studies. The proposed algorithm is called semi-adaptive beamforming (SAB) for subarray-based sensor arrays, which is preliminarily validated through the CPCMA and can also be seen as an improvement of the method in [10].

The major contributions of this paper consists of the following three aspects. Firstly, an alternative adaptive beamforming approach is presented for co-prime arrays, which makes full use of the property of the co-prime arrangement. Secondly, the semi-adaptive beamformer is adapted to the

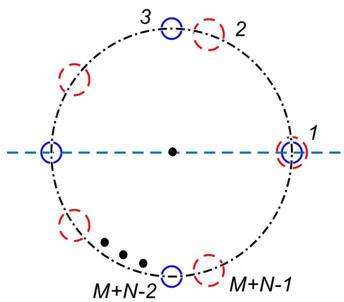

Fig. 1 An eight-element example of the CPCMA arrangement.

CPCMA, achieving optimised beampatterns. Thirdly, the array gain (AG) results across frequencies for typical speech signals are improved, which leads to potential benefits in broadband applications such as speech DOA estimation and speech enhancement.

Section II of this paper formulates the CPCMA recordings and performance metrics of beamformers, including the beampattern and the AG. The proposed SAB approach and its adaption to the CPCMA is described in Section III. Section IV presents experimental results under a number of testing scenarios with conclusions drawn in Section V.

II. The CPCMA Model and Performance Measurements

A. Signal Model

The CPCMA is a type of sparse array, interleaving two uniform circular sub-arrays with M and N microphones, separately ($M > N$; see Fig. 1). M and N are a pair of co-prime numbers, with the only positive integer that divides both being one. The rightmost microphone is seen as the reference, which is shared by two overlapped sub-arrays. Assuming there are K uncorrelated sound sources propagating at the speed of sound (c = 343 m/s) and impinging as plain waves on the CPCMA from diverse DOAs θ_i ($i = 1, 2, \dots, K$), the signal model of the CPCMA recording is expressed as

$$\boldsymbol{y}(t) = \boldsymbol{h}(t) * \boldsymbol{s}(t) + \boldsymbol{v}(t), \tag{1}$$

where $\boldsymbol{y}(t) = [y_1(t), \dots, y_L(t)]^T$ is the array output vector, and $\boldsymbol{s}(t) = [s_1(t), \dots, s_K(t)]^T$, $\boldsymbol{h}(t) = [h_1(t), \dots, h_L(t)]^T$ and $\boldsymbol{v}(t) = [v_1(t), \dots, v_L(t)]^T$ represent source signals, acoustic room impulse responses from the sources to microphones and additive noise, respectively. The noise sensed at each microphone is presumed to be uncorrelated and of same power.

Supposing the reference microphone is located on the x axis of the Cartesian coordinates, the time delay between the i^{th} microphone and the centre is [15]

$$\tau_i = \frac{r}{c}\cos(\theta - \varphi_i), i = 1, 2, \dots, L, \tag{2}$$

where r is the radius of the CPCMA, and φ_i is the angular location of the i^{th} element. Thus, for circular arrangements, the steering vector $\boldsymbol{d}(\omega, \theta)$ of length L can be formulated as

$$\begin{aligned}\boldsymbol{d}(\omega, \theta) &= [e^{-j\omega\tau_1} \quad \dots \quad e^{-j\omega\tau_L}]^T \\ &= \left[e^{-j\frac{\omega r\cos(\theta-\varphi_1)}{c}} \quad \dots \quad e^{-j\frac{\omega r\cos(\theta-\varphi_L)}{c}}\right]^T,\end{aligned} \tag{3}$$

where the superscript T represents the transpose operation, $j = \sqrt{-1}$ is the imaginary unit, and $\omega = 2\pi f$ is the angular frequency corresponding to the temporal frequency f. In addition, the wavelength of the sound source is $\lambda = c/f$.

According to the spatial Nyquist sampling theorem, if the inter-element spacing δ is greater than half of the wavelength, i.e. $\delta > \lambda / 2$, there will be spatial aliasing, where multiple grating lobes occur in the beampattern, having the same power as the main lobe [16]. The operating frequency f_{op_UCA} of a conventionally beamformed uniform circular array (UCA), below which spatial aliasing will not occur, can be found as

$$f_{op\_UCA} = \frac{c}{2\delta} = \frac{c}{4r'\sin\left(\frac{\pi}{M'}\right)}, \tag{4}$$

where r' and M' are the radius and number of microphones, respectively [15]. Additionally, the operating frequency of a CPCMA can be approximated as [9]

$$f_{op\_CPCMA} \approx \frac{c}{4r\sin\left(\frac{\pi}{M \cdot N}\right)}. \tag{5}$$

B. SRP Adjusted DOA Histogram

For both fixed beamformers and adaptive beamformers, two important metrics to evaluate the performance are the beampattern and the array gain [17]. The beampattern illustrates a beamformer's sensitivity to a plane wave impinging on the microphone array. For a conventionally beamformed sub-array of the CPCMA with Q microphones using delay-and-sum (DAS) techniques, it is expressed as [15]

$$\boldsymbol{B}_{DAS}[\boldsymbol{w}_{DAS}(\omega), \theta] = \boldsymbol{w}_{DAS}{}^H(\omega)\boldsymbol{d}(\omega, \theta), \tag{6}$$

where the superscript H represents the Hermitian transpose, and all weights in $\boldsymbol{w}_{DAS}(\omega)$ of length Q are set to $1/Q$, which are the beamforming weights. The beampattern of a sub-array of the CPCMA, processed using the MVDR technique, can be achieved as

$$\boldsymbol{B}_{MVDR}[\boldsymbol{w}_{opt}(\omega), \theta] = \boldsymbol{w}_{opt}{}^H(\omega)\boldsymbol{d}(\omega, \theta). \tag{7}$$

where $\boldsymbol{w}_{opt}$ represents the vector of beamforming weights used in $\boldsymbol{B}_{MVDR}$.

Thus, the beampattern of the CPCMA can be achieved by combining that of the two sub-arrays utilising the product processor, which is [4]

$$\boldsymbol{B}_{CPCMA} = \boldsymbol{B}_{DAS} \times \boldsymbol{B}^*_{MVDR}. \tag{8}$$

Another key measurement is the array gain (AG), which is defined as the ratio between the gain in the direction of the desired signal and the average gain from all undesired directions [17]. The AG can be given by

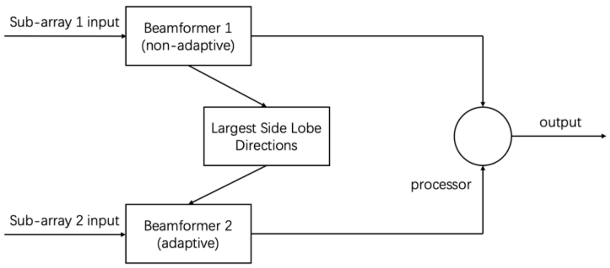

Fig. 2 Work flow of the proposed SAB algorithm

$$D[\boldsymbol{w}(\omega)] = \frac{|\boldsymbol{B}[\boldsymbol{w}(\omega),\theta_s]|^2}{1/\Theta \sum_\theta |\boldsymbol{B}[\boldsymbol{w}(\omega),\theta]|^2}, \tag{9}$$

where θ_s is the steering direction, and Θ is the number of discrete angles utilised in forming the beampattern $\boldsymbol{B}$.

III. Semi-adaptive Beamforming and Its Adaption to CPCMA

Instead of considering the entire array weights, the present study analyses the delay-and-sum beampattern of the *M*-element sub-array to find the directions of grating lobes or largest side lobes $\boldsymbol{\theta_g}(f)$ for each frequency. According to the array signal processing theory, due to spatial aliasing, grating lobes start to occur when the inter-element spacing is equal to or greater than half of the wavelength [16]. If the grating lobes do not occur in the *M*-element sub-array beampattern, the proposed method will then target cancelling the largest side lobes.

Subsequently, the weights of the *N*-element sub-array are achieved dynamically by assuming that virtual sinusoidal interfering sources come from the bearings $\boldsymbol{\theta_g}$, and then setting nulls in these directions utilising adaptive beamforming algorithms. Note that the virtual sinusoidal signals are assumed to have normalised amplitudes and random phases for evaluations in this paper, and their DOAs are arbitrarily configured as $\boldsymbol{\theta_g}$. By combining the two beampatterns via a specific type of co-prime array processor, the grating lobes and large side lobes at $\boldsymbol{\theta_g}$ are expected to be further cancelled compared with the conventional CPCMA, leading to an optimised beamformer. As only one sub-array is processed by the adaptive beamformer, the computational cost of the proposed algorithm can be decreased when compared with state-of-the-art adaptive beamforming approaches for co-prime arrays. Additionally, the SAB is source-independent due to the use of assumed interferences. The work flow of the proposed SAB method is illustrated in Fig. 2.

This paper selects the MVDR approach to process the *N*-element sub-array, which is defined as [8]

$$\min_{\boldsymbol{w}} \boldsymbol{w}^H \boldsymbol{R}_{i+n} \boldsymbol{w} \quad \text{subject to} \quad \boldsymbol{w}^H \boldsymbol{d}(\theta_s) = 1, \tag{10}$$

where $\boldsymbol{w}$ is the weight vector of the *N*-element sub-array at all frequencies, and $\boldsymbol{R}_{i+n}$ represents the interference-plus-noise covariance matrix. $\boldsymbol{d}(\theta_s)$ is the steering vector at the desired source direction, while the superscript *H* denotes the Hermitian transpose operation. The solution of this optimisation problem is [8]

$$\boldsymbol{w}_{opt} = \frac{\boldsymbol{R}_{i+n}^{-1}\boldsymbol{d}(\theta_s)}{\boldsymbol{d}^H(\theta_s)\boldsymbol{R}_{i+n}^{-1}\boldsymbol{d}(\theta_s)}. \tag{11}$$

In practice, $\boldsymbol{R}_{i+n}$ is unavailable, whereas for the proposed algorithm, it can be calculated from the virtual sinusoidal interference and noise signals. Simulations have found that the phase of these undesired signals has no effect on the optimisation result, so they are pre-defined as random-phase signals multiplied by their amplitude, with the steering vector being configured by assuming interferences come from $\boldsymbol{\theta_g}$. Note that the MVDR algorithm used in this paper is nearly identical with the conventional MVDR, whereas the only difference is the assumption of DOAs of virtual interfering sources.

It has been found that a diagonal loading, σ_L^2, of a proper power value can assist with suppressing the interference and noise and narrowing the main lobe of the MVDR approach, [18]. Therefore, the $\boldsymbol{R}_{i+n}$ becomes $\boldsymbol{R}'_{i+n} = \boldsymbol{R}_{i+n} + \sigma_L^2 \boldsymbol{I}$, where I is the unit matrix. As stated in [18], fixed rules for choosing a suitable value of σ_L^2 are hard to achieve and there is a trade-off between minimising the cancellation of the desired signal and restraining the interferences and noise, so an adaptive tuning process of the σ_L^2 is involved in the proposed method. Informal testing found that the σ_L^2 should be selected as approximately one tenth of the diagonal elements in $\boldsymbol{R}_{i+n}$.

Additionally, due to the nature of the MVDR, simulation results show that the amplification of signals at the desired direction will be reduced if the nulls in the beampattern are too close to the main lobe. After a number of tests, the proper threshold is set to 30 degrees. This means if the grating lobes or largest side lobes in the beampattern of the *M* sub-array appear in directions less than 30 degrees, the nulls will be defined at 30 degrees in the *N*-element sub-array beampattern.

A general description of the proposed SAB algorithm is summarised in Table I.

IV. Results and Discussion

A. Experimental Setup

As shown in Table 2, a CPCMA and two contrastive UCAs (UCA-8 with 8 elements and UCA-20 with 20 elements) with the same radius of 0.12 metres are simulated. The conventional CPCMA and the SAB-processed CPCMA have the same array geometry, whereas they employ different beamformers after receiving speech signals that are impinging on the CPCMA. Conventional CPCMAs utilises DAS beamforming techniques, whilst the other employs the proposed SAB beamformer. The product processor is applied to both beamformers to calculate the overall array output after processing the two sub-arrays separately. The performance comparison of the discussed microphone arrays are provided in Section IV.A in terms of the beam pattern and the AG.

TABLE I
THE PROPOSED SAB ALGORITHM

1)	Beamforming the *M*-element sub-array of the CPCMA using conventional DAS ($M > N$) with (6), obtaining the corresponding beampattern $\boldsymbol{B}_{DAS}$.
2)	Searching for grating lobes or largest side lobes in $\boldsymbol{B}_{DAS}$ from -90 to 90 degree relative to the main lobe direction for each frequency, and their directions are labelled as $\boldsymbol{\theta_g}$.
3)	If $\boldsymbol{\theta_g}$ is less than 30 degree, let $\boldsymbol{\theta_g}$ equals 30 degree.
4)	Applying the MVDR method to the other sub-array with (11) by assuming interfering sources come from $\boldsymbol{\theta_g}$, leading to the adaptive beampattern $\boldsymbol{B}_{MVDR}$.
5)	Combining the two sub-array results through a commonly-used processor (the product processor in this paper) with (8), achieving the overall semi-adaptive beampattern of CPCMA $\boldsymbol{B}_{CPCMA}$.

TABLE II
EXPERIMENTAL MICROPHONE ARRAY CONFIGURATIONS

Type of array	Number of elements	Radius (m)	f_{op} (Hz)
CPCMA-8	8	0.12	4567.9
UCA-8	8	0.12	1867.3
UCA-20	20	0.12	4567.9
UCA-5 (Sub-array 1)	5	0.12	1215.7
UCA-4 (Sub-array 2)	4	0.12	1010.6

B. Performance Comparison of Co-prime Beamformers

The aforementioned circular microphone arrays are simulated as per the experimental setup in Section IV.B, and their performances are compared to present the advantage of the SAB beamforming.

Fig. 3 and Fig. 4 illustrate beampatterns of the CPCMA processed by both the DAS and SAB beamformer at example frequencies, which are 1.4 kHz and 3 kHz, with one closed to the operating frequencies of the two sub-arrays and the other higher than twice the two operating frequencies, leading to visible grating lobes in the beampattern. They can represent the performance at low frequencies and high frequencies, respectively. It can be seen that the proposed SAB beamformer uses MVDR as an alternative method to process the second sub-array and achieves optimised beampatterns at both frequencies. Note that this paper focuses on ensuring the beampattern in the forward direction, where the source comes from, is optimal, so only beampatterns in this direction are observed.

At 1.4 kHz, the MVDR method firstly searches for large side lobes in the Sub-array One beampattern, before making comparisons to find the two largest side lobes. Finally, it successfully obtains two nulls at exact directions of these largest side lobes, leading to a much better overall SAB beampattern having a narrower main lobe and smaller side lobes. At 3 kHz, the MVDR also gains two nulls at expected

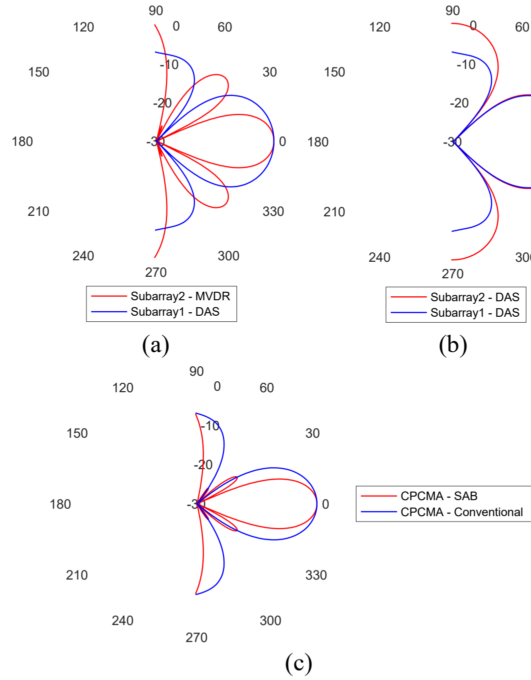

Fig. 3 Beampatterns of the eight-element CPCMA using the conventional beamformer and SAB beamformer, separately: (a) Sub-array beampatterns using the SAB approach; (b) Sub-array beampatterns of the conventional CPCMA; (c) Comparison of beampatterns of the SAB approach and conventional CPCMA. Conditions of simulation: $\theta_s = 0^{\circ}$, f = 1.4 kHz.

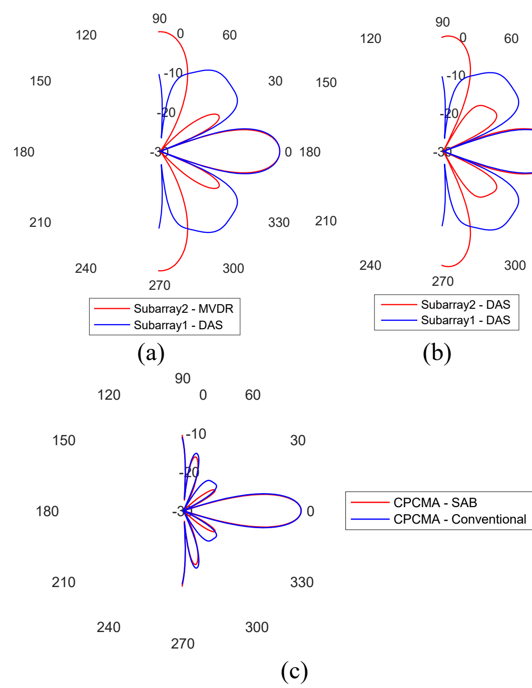

Fig. 4 Beampatterns of the eight-element CPCMA using the conventional beamformer and SAB beamformer, separately: (a) Sub-array beampatterns using the SAB approach; (b) Sub-array beampatterns of the conventional CPCMA; (c) Comparison of beampatterns of the SAB approach and conventional CPCMA. Conditions of simulation: $\theta_s = 0^{\circ}$, f = 3 kHz.

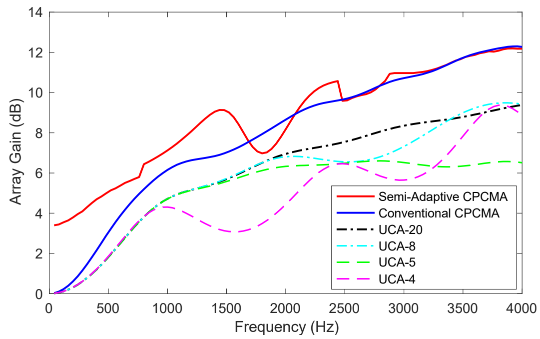

Fig. 5 Comparison of AGs of the CPCMA processed by both beamformers, the contrastive UCAs and the sub-arrays of the CPCMA. Conditions of simulation: $\theta_s = 0^{\circ}$.

positions to cancel the large side lobes in the beampattern of the first sub-array, whereas the conventional DAS beamformer also has nulls at similar bearings. Consequently, the two overall beampatterns are similar, while the SAB beampattern still slightly outperforms that of the conventional beamformer.

In order to look into the performance of SAB to wideband signals, Fig. 5 compares AG results of the SAB-processed CPCMA, the conventional CPCMA, the contrastive UCAs and the two uniform circular sub-arrays of the CPCMA. Generally, the proposed SAB algorithm achieves the highest AG across the frequency band of typical speech signals. Although the SAB result has a small degradation compared with the conventional CPCMA from about 1.6 kHz to 2.1 kHz, it shows significant improvement of AG below 1.6 kHz and is also higher from around 2.1kHz to 2.5 kHz. From 2.5 kHz to 4 kHz, the two curves are quite similar. The two types of CPCMA perform better than all considered UCAs from 0 Hz to 4 kHz in terms of AG. It is worth noting that the proposed approach is the only one that overcomes the problem of low AG below 0.5 kHz. Considering the average AG, the proposed semi-adaptive approach surpasses the conventional CPCMA by around 2 dB, and all the other curves are more than 3 dB below them.

V. Conclusions

This paper proposes a semi-adaptive beamforming approach for co-prime circular microphone arrays. The basic idea is to explore the co-prime property of co-prime arrays and optimise the sub-array weights separately before combining them using a product processor. In this first trial, the MVDR is investigated as an adaptive beamforming method to optimise the weights of one sub-array so that it can cancel the grating lobes or largest sidelobes appearing in the beampattern of the DAS sub-array beamformer. This is achieved by designing the MVDR beamformer to set nulls in the direction of the grating lobes or sidelobes of the other sub-array, which has the potential to decrease the computational complexity and is source-independent due to the usage of assumed sinusoidal signals. Simulation results present the advantage of the SAB approach at improving the beampattern and AG compared with the conventional CPCMA, particularly at low frequencies.

Future work will further investigate potentials of the SAB approach in benefiting co-prime beamforming and its speech processing applications, such as DOA estimation, source separation, speech enhancement, etc. Possible directions are: 1) exploring the results of beamforming the N-element sub-array with adaptive approaches according to the DAS beampattern of the M-element sub-array, and comparing them with the results in this paper; 2) evaluating various target directions and optimising sub-array weights of the CPCMA for these cases to further develop the SAB application, after which other metrics such as Perceptual Evaluation of Speech Quality (PESQ) and Source to Distortion Ratio (SDR) can also be used by simulating audio recordings to check whether the overall audio quality is improved; 3) instead of configuring a threshold, finding better solutions for cases when grating lobes or largest side lobes are too close to the main lobe of the DAS sub-array beampattern.

References

[1] V. Trees, *Optimum Array Processing*. New York, USA: Wiley, 2002.

[2] P. P. Vaidyanathan and P. Pal, "Sparse Sensing with Coprime Arrays," *the Forty-Fourth Asilomar Conference on Signals, Systems and Computers*, pp. 1405-1409, 2010.

[3] J. Benesty, J. Chen, and Y. Huang, *Microphone Arrays Signal Processing*. Berlin, Germany: Springer-Verlag, 2008.

[4] J. Zhao and C. Ritz, "Investigating Co-Prime Microphone Arrays for Speech Direction of Arrival Estimation," *Asia-Pacific Signal and Information Processing Association Annual Summit and Conference (APSIPA ASC 2018)*, pp. 1658-1664, November 2018.

[5] N. Xiang, D. Bush, and J. E. Summers, "Experimental Validation of a Coprime Linear Microphone Array for High-resolution Direction-of-arrival Measurements", *The Journal of the Acoustical Society of America*, vol. 137, issue 4, pp. 261-266, April 2015.

[6] J. Ramirez and J. Krolik, "Multiple Source Localization with Moving Co-prime Arrays", *IEEE International Conference on Acoustics, Speech and Signal Processing (ICCASP 2015)*, pp. 2374-2378, April 2015.

[7] Q. Shen, W. Liu, W. Cui, S. Wu, Y. D. Zhang, and M. G. Amin, "Low-complexity Direction-of-arrival Estimation Based on Wideband Co-prime Arrays," *IEEE/ACM Transactions on Audio, Speech, and Language Processing*, vol. 23, issue 9, pp. 1445-1456, September 2015.

[8] I. M. Rooney and J. R. Buck, "Spatial Power Spectral Density Estimation Using a Welch Coprime Sensor Array Processor", *The Journal of the Acoustical Society of America*, vol. 145, issue 4, pp. 2350-2362, April 2019.

[9] J. Zhao and C. Ritz, "Co-prime Circular Microphone Arrays and Their Application to Direction of Arrival Estimation of Speech Sources", *IEEE International Conference on Acoustics, Speech and Signal Processing (ICCASP 2019)*, pp. 800-804, May 2019.

[10] K. Adhikari, "Beamforming with Semi-Coprime Arrays," The Journal of the Acoustical Society of America, vol. 145, issue 5, pp. 2841-2850, May 2019.

[11] J. Zhao and C. Ritz, "Semi-Coprime Microphone Arrays for Estimating Direction of Arrival of Speech Sources", *Asia-Pacific Signal and Information Processing Association Annual Summit and Conference (APSIPA ASC 2019)*, November 2019.

[12] Y. Gu, C. Zhou, N. A. Goodman, W. Song, and Z. Shi, "Coprime Array Adaptive Beamforming Based on Compressive Sensing Virtual Array Signal", *IEEE International Conference on Acoustics, Speech and Signal Processing (ICCASP 2016)*, pp. 2981-2985, March 2016.
[13] C. Liu and P. P. Vaidyanathan, "Coprime Arrays and Samplers for Space-time Adaptive Processing", *IEEE International Conference on Acoustics, Speech and Signal Processing (ICCASP 2015)*, pp. 2364-2368, April 2015.
[14] C. Zhou, Y. Gu, S. He, and Z. Shi, "A Robust and Efficient Algorithm for Coprime Array Adaptive Beamforming", *IEEE Transactions on Vehicular Technology*, vol. 67, issue 2, pp. 1099-1112, February 2018.
[15] J. Benesty, J. Chen, and I. Cohen, *Design of Circular Differential Microphone Arrays*. Switzerland: Springer International Publishing, 2015.
[16] W. L. Stutzman and G. A. Thiele, *Antenna Theory and Design*. *3*rd ed., New York: Wiley, 2013, pp. 307.
[17] H. Cox, R. Zeskind, and M. Owen, "Robust Adaptive Beamforming," *IEEE Transactions on Acoustics, Speech, and Signal Processing*, vol. 35, issue 10, pp. 1365-1376, 1987.
[18] T. S. J. Laseetha and R. Sukanesh, "A Novel Robust Adaptive Beamformer using Diagonal Loading", *International Journal of Computer Applications*, vol. 9, issue 5, pp. 35-40, April 2011.